Nonlinear Optical Property Measurement in Integrated Photonic Devices

Erik Benkler, Anatoly Sherman, and Harald R. Telle

Abstract — We discuss and demonstrate a novel technique for the measurement of nonlinear optical parameters related to the complex third-order susceptibility $\chi^{(3)}$, such as nonlinear refractive index, two-photon absorption coefficient, and nonlinear figure of merit. The method is ideally suited for the spatially resolved measurement of such properties along a waveguide path ("photonic bus") inside integrated photonic devices.

Index Terms — integrated photonic devices, measurement techniques, nonlinear optics

1. INTRODUCTION

NONLINEAR effects provide the foundation for the implementation of any direct opto-optical function in integrated photonic devices [1]. Several functional building blocks like all-optical switches or modulators based on nonlinear interactions between two or more independent optical fields can be integrated into a photonic chip. These units are interconnected by waveguides, either intra-chip or inter-chip, and even over very long distances via optical fibers. Hence, on the one hand, nonlinear effects are desired in the functional units. On the other hand they are usually unwanted in the waveguides used for interconnection. As an example channel crosstalk due to four wave mixing is an unwanted effect for WDM transmission.

Novel nonlinearity measurement techniques are required for the characterization of integrated photonic devices, with the following demands: First, the technique must be applicable to waveguides which transmit a single transverse mode. This excludes standard techniques like z-scan [2] relying on transversal effects. Second, it should provide spatial resolution better than a few ten µm along the photonic bus. Third, the method must be highly sensitive in view of the short interaction lengths required for the spatial resolution mentioned above. Here, we discuss a novel technique which fulfills these requirements.

Manuscript received March 31, 2011. This work was supported in part by the German Research Foundation DFG within the framework of Collaborative Research Center SFB407.

E. Benkler (e-mail: Erik.Benkler@ptb.de) and H.R. Telle are with the Physikalisch-Technische Bundesanstalt (PTB), Bundesallee 100, D-38116 Braunschweig. A. Sherman is with the aleo solar AG, Osterstrasse 15, D-26122 Oldenburg.

This paper is organized as follows: First, the basic technique employed for the nonlinearity measurement is described where emphasis is put on referencing the nonlinear parameters of the waveguide under test to well-known optical properties of a bulk sample. Its outstanding sensitivity is demonstrated using a sample with extremely small nonlinearity. Then, the method is extended to complex quantities, i. e. to the simultaneous measurement of the real and imaginary components of the third-order susceptibility $\chi^{(3)}$, yielding a direct measurement of the nonlinear figure of merit which plays an important role for all opto-optical functions. Finally, an outlook is given how a modification of the method can provide the required spatial resolution along the photonic bus.

2. MEASUREMENT PRINCIPLE

For the measurement of $\chi^{(3)}$ nonlinearities in integrated photonic devices a $\chi^{(3)}$ effect compatible with their waveguide geometry must be used. For this reason, we employ collinear nearly degenerate four wave mixing, which was sometimes termed three wave mixing in the literature [3]. In a special case of this process, mixing fields E_{m1} and E_{m2} at new frequencies $\nu_{\mathrm{m1}} = 2\nu_1 - \nu_2$ and $\nu_{\mathrm{m2}} = 2\nu_2 - \nu_1$ are generated from two excitation fields E_1 and E_2 with optical frequencies ν_1 and ν_2 (see inset of Fig. 1) The mixing fields carry the information on both the real and imaginary parts of $\chi^{(3)}$:

$$E_{\mathrm{m1}} \propto \chi^{(3)} E_1^* E_1 E_2 \qquad (1)$$

The mixing field can be heterodyne detected, which has two major benefits:

1. It enables, in principle, shot noise limited detection sensitivity due to heterodyne gain
2. The mixing field is detected, i.e. its phase and its amplitude, ultimately allowing the measurement of both real and imaginary part of $\chi^{(3)}$.

Fig. 1 schematically shows the experimental setup. A modelocked Er-fiber laser with central wavelength of λ = 1580 nm, a pulse length of τ = 100 fs, a repetition rate f_{rep} = 56 MHz, and average power of 10 mW is used as light source.

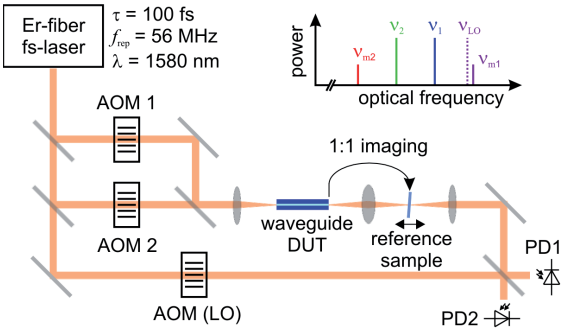

Figure 1: Experimental setup. See text for details. The inset shows a stick frequency diagram for illustration of the heterodyne detection of nearly degenerate four wave mixing signals.

The modelocked laser generates an optical frequency comb, i.e. its spectrum consists of sharp equidistant lines. In the strict sense this fact should be taken into account in the explanation of the four wave mixing process. However, it turns out that this does not lead to substantially different results than just considering cw fields instead, as long as the pulse peak power remains approximately constant during propagation inside the device under test (negligible losses and dispersion effects). Hence for simplicity, the discussion throughout this paper is restricted to one comb tooth.

The laser output is split up into three arms and the optical frequencies in each arm are shifted by means of acousto-optical modulators (AOMs).

In the first two arms, the four-wave mixing excitation fields E_1 and E_2 are generated and subsequently overlapped in space and time at a beam combiner. The excitation fields are thus co-propagating and can hence be coupled into the waveguiding device under test (DUT). In the DUT, the fields E_{m1} and E_{m2} are generated by collinear nearly degenerate four wave mixing. In principle, the detection of one of these fields would be enough to gain the desired information on the third-order susceptibility.

However, the mixing field critically depends on the peak power and other excitation pulse parameters which might even fluctuate during a measurement. For this reason, we introduced a novel method which is based on referencing the mixing field to the mixing field generated by the same excitation pulses and under equal experimental circumstances in an additional reference sample [4]. For this purpose, the output facet of the waveguide DUT is imaged 1:1 to an imaging plane by means of two parabolic mirrors (shown as a single lens in Fig. 1). A thin bulk reference sample with well known optical properties is introduced in the vicinity of the beam waist at the imaging plane. The overall mixing field thus consists of the sum of the mixing fields generated in the waveguide DUT and in the reference sample. Due to the 1:1 imaging, the mode field diameter (MFD) at the beam waist is identical with the MFD in the waveguide. Hence, if the reference sample is located in the beam waist, the two complex valued contributions to the detected mixing product add-up, whereas contributions from the reference sample can be neglected if the reference is far from the beam waist since the MFD is much larger than at the output facet of the DUT. The reference sample can be continuously moved into and out of the beam waist, with a minimum of disturbances, e.g. due to beam geometry changes. Using this principle, the nonlinear parameters of the DUT can be referenced to the parameters of the well-characterized reference sample, in particular without any knowledge of the exact pulse parameters or mode field diameters.

One of the generated mixing fields is then heterodyne detected. For this purpose, the mixing field is spatio-temporally superimposed with an auxiliary "local oscillator" field E_{LO} generated by frequency shifting the optical frequency in the third arm to ν_{LO} (see stick diagram in the inset of Fig. 1). The resulting beat photocurrent at the frequency $\nu_{beat} = \nu_{m1} - \nu_{LO}$ is then detected with photodiode PD1:

$$i_{beat} \propto E_{m1} E_{LO}^{*} + \text{c.c.} \qquad (2)$$

Detecting both quadratures, or in other words both amplitude and phase, of the beat photocurrent allows the determination of both the real and the imaginary part of the third-order susceptibility $\chi^{(3)}$. The two quadratures are detected with a two-phase lock-in amplifier. For the lock-in detection an electrical reference signal at the beat frequency ν_{beat} is required. Its amplitude should be constant and its phase must have a strict relation to the phases of the excitation and LO fields. Ideally, it should be independent of any length fluctuations of either arm of the nested Mach-Zehnder interferometers. This can be achieved by detecting the two beat-notes $E_1 E_2$ and $E_{LO} E_1$ with the help of PD2. The corresponding RF beat frequencies are $\nu_{b1} = \nu_1 - \nu_2$ and $\nu_{b2} = \nu_{LO} - \nu_1$. These RF beat signals are individually phase-tracked by two separate phase locked loops (PLLs). Subsequently, the PLL output signals are mixed using a double-balanced mixer, yielding the desired reference signal at $\nu_{ref} = \nu_{b1} - \nu_{b2} = \nu_{beat}$. This scheme common-mode rejects perturbations due to arm length fluctuations in the interferometers to a high degree without the need for any active stabilization.

3. *Demonstration of Sensitivity*

In this section, we use a sample with purely real $\chi^{(3)}$, i.e. negligible two-photon absorption for a demonstration of the extreme sensitivity of the described heterodyne detection technique. A

purely real $\chi^{(3)}$ is well approximated in fused silica based DUTs. In this case, the amplitude of the beat photocurrent is proportional to Re($\chi^{(3)}$). As a waveguide DUT, we use a 2.1 cm short piece of NKT photonics HC-1550-01 hollow-core photonic crystal fiber (HC-PCF). In HC-PCFs the huge majority of light is confined to the hollow, air-filled core based on the photonic bandgap resulting from the photonic crystal cladding structure around the core. Owing to the very small light - fused silica overlap, these fibers have an effective nonlinearity which is about 3 orders of magnitude smaller than in standard solid core fibers. To appreciate the high sensitivity of the method, it is demonstrative that usual fiber nonlinearity measurements require kilometers long fibers instead of the few cm of HC-PCF investigated here. As a reference sample a 25 µm thin fused silica plate is employed. Its thickness is much smaller than the confocal parameter (180 µm) of the beam.

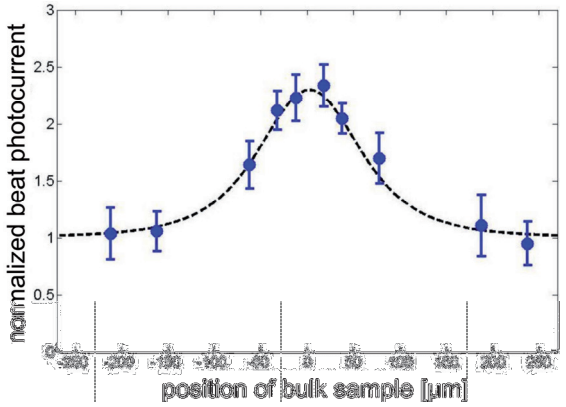

Figure 2: Beat photocurrent amplitude $|i_{beat}|$ as the reference sample is moved through the imaging plane, normalized to the beat photocurrent resulting from the HC-PCF alone. Blue circles: Experiment, dashed line: Calculation with a Gaussian beam.

Fig. 2 shows the result of a measurement in which the reference sample was shifted through the beam waist at the imaging plane. Please notice that although a sample is scanned through a focused beam, the method relies on a completely different principle than the z-scan technique. The dashed theoretical curve is computed for the 25 µm thin fused silica assuming a Gaussian beam with a confocal parameter of 180 µm, corresponding to the 13 µm MFD of the HC-PCF. From the normalized value at maximum (reference in focus), the value for the effective nonlinear refractive index of the HC-PCF is derived to be $n_2^{\text{HC-PCF}} = (5.7 \pm 3.2) \times 10^{-4} n_2^{\text{fused silica}}$, taking into account the (measured) attenuation of the excitation fields between the DUT and reference sample. In absolute terms, the cross-phase-modulation amplitude in the HC-PCF was about 10^{-5} rad.

This experiment demonstrates the potential of the technique for nonlinearity measurements in short waveguide DUT, such as integrated photonic devices.

4. Complex $\chi^{(3)}$ measurement

As described in section 2, the technique provides information on both real and imaginary part of $\chi^{(3)}$. The real part as measured with our technique is related to the nonlinear refractive index (using SI units):

$$n_2 = \frac{3}{2\varepsilon_0 n_0^2 c} \mathrm{Re}\left\{\chi^{(3)}\right\}, \tag{3}$$

and the imaginary part is related to the two-photon absorption coefficient:

$$\beta = \frac{3\pi}{\varepsilon_0 n_0^2 c \lambda} \mathrm{Im}\left\{\chi^{(3)}\right\}. \tag{4}$$

For opto-optical functions like all-optical switches, it is beneficial to have a large nonlinear refractive index and small linear and nonlinear absorption. For this reason, a nonlinear figure of merit can be defined as [5]

$$NFOM = \frac{n_2}{\lambda\beta} = \frac{\mathrm{Re}\left\{\chi^{(3)}\right\}}{2\pi\,\mathrm{Im}\left\{\chi^{(3)}\right\}}. \tag{5}$$

A value of $NFOM > 1$ is widely used as criterion for the suitability of a material for all-optical switching devices. Our technique directly measures the complex value of $\chi^{(3)}$. Hence, the $NFOM$ is also directly determined with real and imaginary part of $\chi^{(3)}$ measured coequally. Usually, this is not the case, since different measurement or analysis techniques are used for the nonlinear refractive index and for the two-photon absorption coefficient.

For a demonstration, we measured the complex value of $\chi^{(3)}$ of a crystalline <100> oriented silicon plate with a thickness of 41.5 µm. In this experiment, the roles of the waveguide and bulk sample have been exchanged, i.e., a standard single mode fiber (SMF28) with a length of 13.5 mm was used as waveguide sample acting as reference, and the bulk silicon plate as DUT was scanned through the imaging plane. We measured both quadratures of the beat photocurrent with a lock-in amplifier as described in section 2, for two cases:

1. The Si bulk sample is positioned far out of focus, i.e. the detected signal consists of the contribution from the SMF28 fiber alone.
2. The Si bulk sample is positioned in the imaging plane, i.e. the detected signal consists of the contributions from both samples.

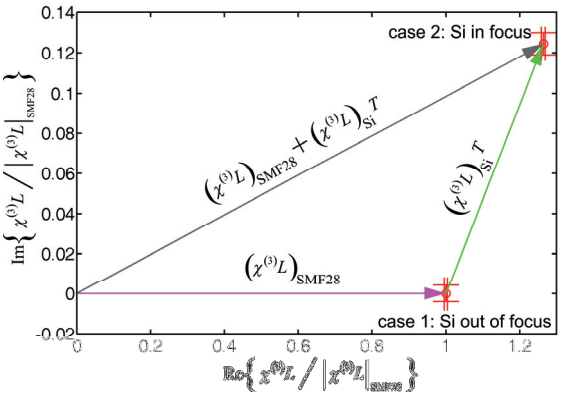

Figure 3: Normalized complex measurement data plotted in the complex plane. Magenta vector: Case 1 (Si plate out of focus, purely real contribution from SMF28 only), gray vector: Case 2 (Si plate in focus, contributions from both samples), green vector: Contribution of the Si plate. T is the transmission through the 1:1 imaging system.

For the analysis, we plot the measured quadratures as vectorial components into a Cartesian coordinate system. Since the SMF28 fiber has negligible two-photon absorption at telecom wavelengths, we can rotate this coordinate system such that the measurement point for case 1 (bulk sample out of focus) is on the abscissa. It can be shown [6] that the abscissa then describes the real part, and the ordinate describes the imaginary part of $\chi^{(3)}L$, where L is the sample length. We normalize the data to $\left|\chi^{(3)}L\right|_{\mathrm{SMF28}}$ as shown in Fig. 3.

From this plot, the $NFOM_{\mathrm{Si}}$ of silicon can be directly derived, even without knowledge of the Si plate thickness: It is simply given by the abscissa divided by the ordinate of the green vector in Fig. 3, divided by 2π. We find $NFOM_{\mathrm{Si}} = 0.34$, which is in good accordance with literature values. Given the lengths of the samples, we determine a nonlinear refractive index of $n_2^{\mathrm{Si}} = 3.4\times10^{-18}\ \mathrm{m^2/W}$ and a two-photon absorption coefficient of $\beta_{\mathrm{Si}} = 6.1\times10^{-12}\ \mathrm{m/W}$.

5. Outlook: Spatially Resolved Technique

With the described technique of co-propagating excitation pulses, the four wave mixing signal is generated continuously at all positions along the waveguide. In chapter 3 we demonstrated the high sensitivity of the technique, which allows to measure third-order nonlinearities of fused silica samples as short as a few micrometers. This means that the sensitivity of the method is compatible with a spatial resolution of a few micrometers along the propagation direction. However, to achieve such a resolution, the method must be modified.

The basic idea is to send two excitation pulses with frequencies ν_1 and ν_2 through a DUT's waveguide path from opposite directions as illustrated in Fig. 4.

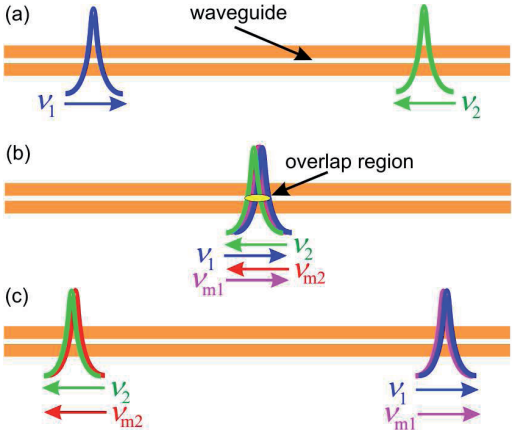

Figure 3: Basic principle of the spatially resolved technique. Excitation pulses (see stick diagram in the inset of Fig. 1 for the involved frequencies) are sent into a waveguide path from opposite ends. (a) Situation before the pulses encounter each other: No nonlinear interaction. (b) Whilst the counter-propagating excitation pulses overlap, counter-propagating four wave mixing pulses are generated. The overlap region is defined by the length of the pulses. (c) After the nonlinear interaction, the four wave mixing pulses can be heterodyne detected. See text for more details.

The pulses travel through the waveguide, and before they encounter each other, they cannot interact (Fig. 4(a)). However, at a position along the waveguide path, which is well-defined and controllable by the relative timing of their entrance into the device and by their group velocities, the excitation pulses overlap (Fig. 4(b)). The length of the overlap region is defined by the length of the pulses. For 100 fs short pulses, this length is of the order of a few ten micrometers. Whilst the pulses overlap, they interact through a four wave mixing process. As a result, counter-propagating mixing pulses are generated. After the overlap (Fig. 4(c)), they co-propagate with one of the excitation fields, respectively, and can thus be heterodyne detected as described in the previous sections. This approach is limited by several factors: In presence of chromatic dispersion, the pulses are stretched before the interaction as they travel through the waveguide. This limits the spatial resolution. Furthermore, the referencing to a bulk sample method relies on the assumption that the MFD in the waveguide device is constant along the path. This fact can, however, be exploited as well: If the MFD changes along the waveguide, as e.g. in an integrated photonic circuit, or at a splice between fibers with different core diameters, this position can be measured with high spatial resolution.

As mentioned before, the sensitivity of the measurement technique is high enough to measure four wave mixing fields generated in interaction regions as short as a few micrometers, i.e. shorter than the overlap region of 100 fs short pulses. Another benefit of the approach to couple the excitation fields in from two sides is that in this way, a certain waveguide path can be addressed amongst a manifold in integrated photonic circuits.